Optical and Quantum Electronics (2022) 54:854
https://doi.org/10.1007/s11082-022-04267-6

Synthesis and augmented optical characteristics of PEO–PVA–$SrTiO_3$–NiO hybrid nanocomposites for optoelectronics and antibacterial applications

Shaimaa Mazhar Mahdi[1] · **Majeed Ali Habeeb**[1]

Received: 26 August 2022 / Accepted: 1 October 2022 / Published online: 22 October 2022

Abstract
Recently, polymer composite materials have done well in a wide range of technological applications, such as renewable energy, biomedical applications, optoelectronic devices… etc. In this study, the researchers study structural and optical properties of PEO–PVA blend doped with different weight percentages of $SrTiO_3$–NiO NPs (0, 1, 2, 3 and 4) wt% which were obtained via the solution casting method. Scanning electron microscopy results show that the grain aggregates as the concentration of nanoparticles increases and surface morphology of the NCs with many groupings or pieces randomly doled out on the surface coherent and homogeneous. Optical microscope images show that the additive distribution of NPs in the blend was homogeneous and the nanoparticles create a continuous network inside the polymers. The transmittance of PEO–PVA–$SrTiO_3$–NiO NCs is decreased from 46 to 21% when the concentrations of $SrTiO_3$–NiO NPs reached 4%.The allowed and forbidden indirect energy gap of this NCs decreased from 3.6 to 2.5 (eV), and from 3.8 to 2.5 (eV), respectively, when increasing the weight percentages of NPsto 4 wt%. This behavior is useful for optoelectronics, solar cells, and diodes fields with low cost and light weight. The absorption, absorption coefficient, extinction coefficient, refractive index, real and imaginary dielectric constants and optical conductivity of PEO–PVA blend increases with increasing the concentration of $SrTiO_3$–NiO NPs. The inhibition zone values of *E. coli* and *S.* aureusmicro-organisms increased by increasing the $SrTiO_3$–NiO NPs ratio in PEO–PVA to 28 and 24 mm. Thus, these results indicate the applicability and potential of the nanocomposites for use in optoelectronics and medical applications.

Keywords PEO–PVA · $SrTiO_3$–NiO NPs · Optical properties · Antibacterial activity

✉ Majeed Ali Habeeb
pure.majeed.ali@uobabylon.edu.iq

Shaimaa Mazhar Mahdi
alshamarish825@gmail.com

[1] Department of Physics, College of Education for Pure Sciences, University of Babylon, Hillah, Iraq

1 Introduction

Mixing polymers is a key step in making new polymeric materials which can be used in many ways. Polymer blends have many benefits, but the most important is that the qualities of finished product can be altered to suit requirements of various applications in a manner not achievable with single polymers. Polymer nanocomposites have just recently been found to be useful in a wide range of scientific fields. Because of this, new technologies have been made. This is because adding nanoparticles to a polymer matrix has a big effect on the material's thermal, optical, and electrical characteristics, even though the material still has its own qualities and characteristics. This is because adding nanoparticles to a polymer matrix changes the thermal, optical, and mechanical characteristics of the material in a big way (Chang et al. 2008). When studying electronic transitions, the optical properties of polymers are important because they can be used as optical filters, cover insulators, selection surfaces, and green homes, among other things (Luo et al. 2013). Polymer optical characteristics, on the other hand, are designed to improve reflection, antireflection, interference, and polarization qualities. Because of its remarkable thermal stability, PEO is an intriguing basis material. PEO is a semi-crystalline polymer that can exist in both solid and liquid form.at ambient temperature, amorphous and crystalline phases (Hayder et al. 2020). PVA is one of the most significant polymeric compounds since it has many industrial uses and is very affordable to create. PVA is a crystalline polymer which is extremely soluble in water; nevertheless, dissolving it necessitates the breakdown of the crystal structure, which must be done at a high temperature (Kumar et al. 2015). $SrTiO_3$ has been demonstrated to have persistent photoconductivity, which means that exposing the crystal to light increases its electrical conductivity by more than two orders of magnitude. The improved conductivity lasts for several days after the light is switched off, with negligible degradation (Pattabi et al. 2007). NiO is a transition metal oxide which has a cubic lattice structure. It has gained prominence due to its potentials. There are applications in numerous fields, such as catalysis. With the advancement of every industry and technology, the focus has shifted to nanoscale materials because this length scale requires additional qualities (Chandrakala et al. 2014). Optical engineering has evolved to be based on precision optical products as a result of the development of laser and optoelectronic technology. The subjects of information science, energy science, material science, life science, space science, precision manufacturing, computer science, and microelectronics technology are now linked disciplines that closely straddle and encroach upon one another. It encompasses several important developing fields, including optical information processing, optical storage and recording, laser technology, and optical communication (McKee et al. 1998). Since the emergence of infections which are resistant to antibiotics is hardly keeping up with the discovery of new antimicrobial medications, developing effective antibiotic substitutes has attracted more attention due to these and other factors. Utilizing nanoparticles with antibacterial properties and nanostructures with anti-adhesive activities against biofilms is a viable method (Abutalib and Rajeh 2021; Alghamdi et al. 2022a, b). The efficiency of composites' production is significantly impacted by the usage of these nanoparticles, which enhance the chemical and antimicrobial processes inside them. There have not been many researches, nevertheless, on how nanomaterials affect the performance characteristics of an enhanced composite. $SrTiO_3$–NiO has an antibacterial effect on bacteria without producing dangerous biocides. To our knowledge, no attempt has been made to synthesize nanocomposites

including $SrTiO_3$–NiO nanoparticles. The purpose of this study is to present of the low-cost and easy synthesis process by PEO–PVA–$SrTiO_3$–NiO nanocomposites for opto-electronics and antibacterial applications.

2 Materials and methods

The casting procedure was used to make f PEO–PVA–$SrTiO_3$–NiO nanocomposites. Casting method has many advantages: it can be easily used in laboratories, the solution may either spread on a substrate or cast into a mold, an additive can be easily added and the properties of polymer composites can be easily identified, a liquid on a surface is dried without any external factor such as thermal or mechanical stress, offers a variety of additive options to the polymer, the additive can be added to any polymer–solvent solution, polymer films formed through solvent casting method usually have thicknesses which are homogeneously distributed and produces clear films of higher optical clarity. The films were prepared by dissolving 1 gm of (PEO–PVA) blend with 50/50% in Using a magnetic stirrer, stir 40 ml of distilled water for 45 min. at temperature 70 C to create a more uniform solution. $SrTiO_3$ and NiO nanoparticles are mixed with polymers at various concentrations of 0, 1, 2, 3, and 4 weight percent. The solution was kept in a petri dish. Polymer mix nanocomposites were created after 4 days of room temperature progressive drying of the fluid. The petri dish's PEO–PVA–$SrTiO_3$–NiO NCs were cut out and utilized for analysis. The optical characteristics of PEO–PVA–$SrTiO_3$–NiO NCs were investigated using a double beam spectrophotometer (Shimadzu, UV-18000A) at wavelengths ranging between 200 and 800 nm, and a test for samples in different concentrations was performed using an Olympus type Nikon-73346 optical microscope with a magnifying power of (10x) and equipped with a camera for microscopic photography. The antimicrobial activity of the nanocomposite films against two clinical bacteria, *Escherichia coli* and *Staphylococcus aureus*.

Equation-defined absorption coefficient (α) for nanocomposites (Gautam and Ram 2010)

$$\alpha = 2303\,A/t \tag{1}$$

A is the absorbance of the sample, and t is its thickness.

For calculating the energy gap, the following equation was employed (Blythe and Bloor 2005; Goswami et al. 2017)

$$\alpha h\upsilon = B\,(h\upsilon - Eg)^{r} \tag{2}$$

B is constant, hυ indicates photon energy, Eg indicates optical energy band gap, r = 2, or 3 for allowed and forbidden indirect transition.

Refractive index (n) of PEO–PVA–$SrTiO_3$–NiO NCswas calculated by using the equation (Shankar et al. 2014)

$$n = \left(1 + R^{1/2}\right)/\left(1 - R^{1/2}\right) \tag{3}$$

Following equation was used to compute the extinction coefficient (k) (Mahdi and Habeeb 2022)

$$k = \alpha\lambda/4\pi \tag{4}$$

Real and imaginary (ε_1 and ε_2) components of the dielectric constant were computed (Selvi et al. 2017)

$$\varepsilon_1 = n^2 - k^2 \tag{5}$$

$$\varepsilon_2 = 2nk \tag{6}$$

Optical conductivity was estimated using the equation below (Tintu et al. 2010)

$$\sigma = \frac{\alpha nc}{4\pi} \tag{7}$$

where: c is the velocity of light.

3 Results and discussions

3.1 Scanning electron microscope (SEM) measurements of PEO–PVA–$SrTiO_3$–NiO NCs

Figure 1 displays a SEM image at different doses of NPs, of the surface of a pure and filled polymer film (0, 1, 2, 3, and 4) wt% of the blend. The image of pure blend PEO–PVA in Fig. 1a shows morphological structure which has numerous crystalline domains i.e. spherules. Adding of $SrTiO_3$–NiO nanoparticles to the pure reduces the size of spherules significantly, and the surface morphology improves from rough to relatively smooth, as illustrated in Fig. 1b for PEO–PVA–$SrTiO_3$–NiO nanocomposites. A smooth look is usually related to a decrease in the crystallinity of the PEO–PVP blend. Furthermore, the surface is completely filled with pores, where their distribution becomes denser due to an aggregation of $SrTiO_3$–NiO nanoparticles because of spherule shrinkage, pores form between nanoparticles and polymer blend surfaces, and are regarded a sort of complexation/miscibility between PEO–PVA blend and $SrTiO_3$–NiO nanoparticles. Furthermore, these pores correlate to polymer linked networks. The increase in porosity has been attributed to an increase in free ion production and thus, an increase in ionic conductivity. The number of pores in nanocomposites is greatly reduced due to aggregation of $SrTiO_3$–NiO nanoparticles, as displayed in Fig. 1c, d, due to the presence of structural rearrangement by an, which allows $SrTiO_3$–NiO nanoparticles to combine. PEO–PVA $SrTiO_3$–NiO nanocomposites, the pores are practically invisible, as illustrated in Fig. 1e when 4 wt% $SrTiO_3$–NiO nanoparticles are added to PEO–PVA (Jebur et al. 2020a).When $SrTiO_3$–NiO nanoparticlesratio gradually growing in PEO–PVA blend, appearance of several spherical particle aggregates or chunks on the surface of nanocomposites indicates the presence of a homogenous growth mechanism. It gets softer as the concentration of both particles increases, where nanoparticles aggregate and are well distribution in PEO–PVA blend form a continuous network with in the polymers (Jebur et al. 2020b).

3.2 Optical Microscope for PEO–PVA–$SrTiO_3$–NiO NCs

Figure 2 displays optical microscope images for PEO–PVA–$SrTiO_3$–NiO NCs films. Different concentrations were taken for specimens. Magnification strength (10X) nonetheless, as shown in the images, there is a clear difference between the samples (a- b- c- d- and e). When to increasing ratiosof $SrTiO_3$–NiO NPsin PEO–PVA blend, the NPs create a continuing network inside the polymers, reaching to 4 wt% for PEO–PVA–$SrTiO_3$–NiO

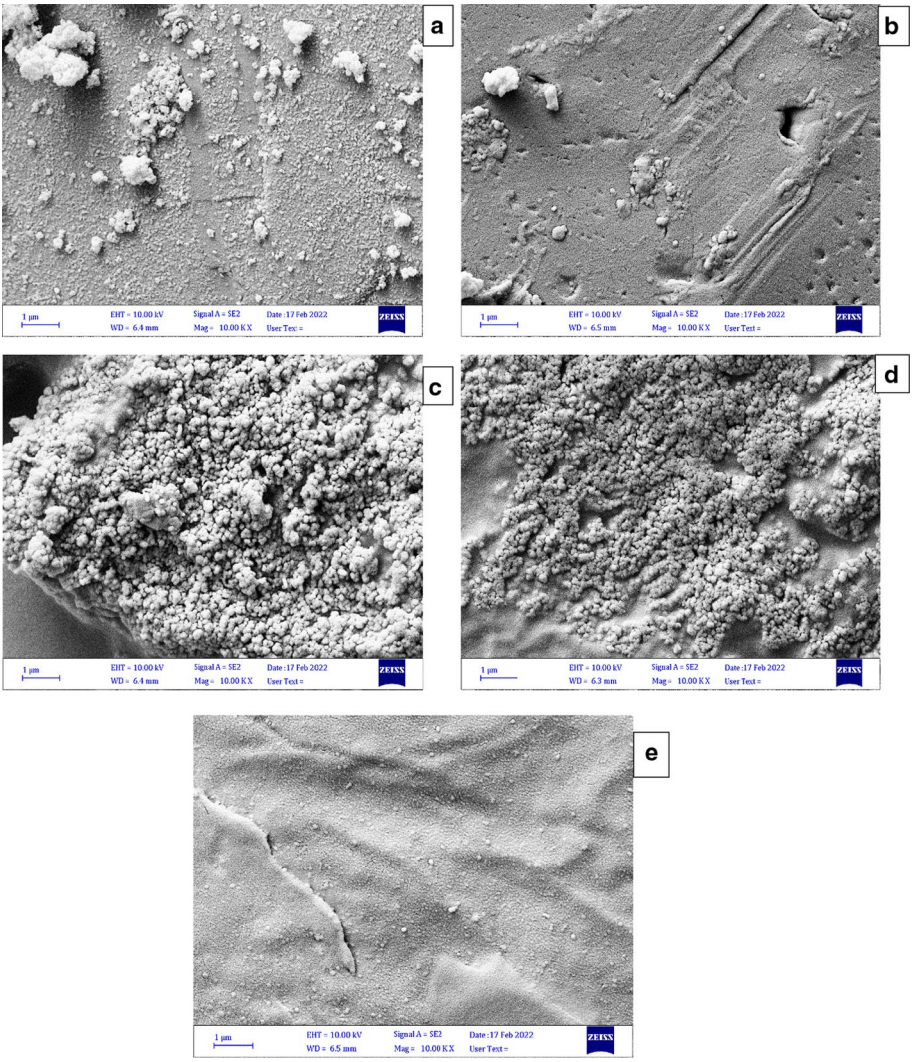

Fig. 1 SEM images 1 µm for PEO–PVA–$SrTiO_3$–NiO NCs: **a** for pure **b** for 1 wt% $SrTiO_3$–NiO NPs, **c** for 2 wt% $SrTiO_3$–NiONPs, **d** for 3 wt% $SrTiO_3$–NiONPs, **e** for 4 wt% $SrTiO_3$–NiONPs

nanocomposites. This network is made up of indoor routes, and nanocomposites allow charging carriers to move through such pathways (Habeeb and Hashim 2020; Habeeb 2011).

3.3 The Optical Characteristics for PEO–PVA–$SrTiO_3$–NiO NCs

Figure 3 shows the relationship between optical absorbance and wavelength for PEO–PVA–$SrTiO_3$–NiO NCs. PEO–PVA exhibits significant radiation absorption in the wavelength range 200–400 nm. The spectra suggest that all of these films have a higher

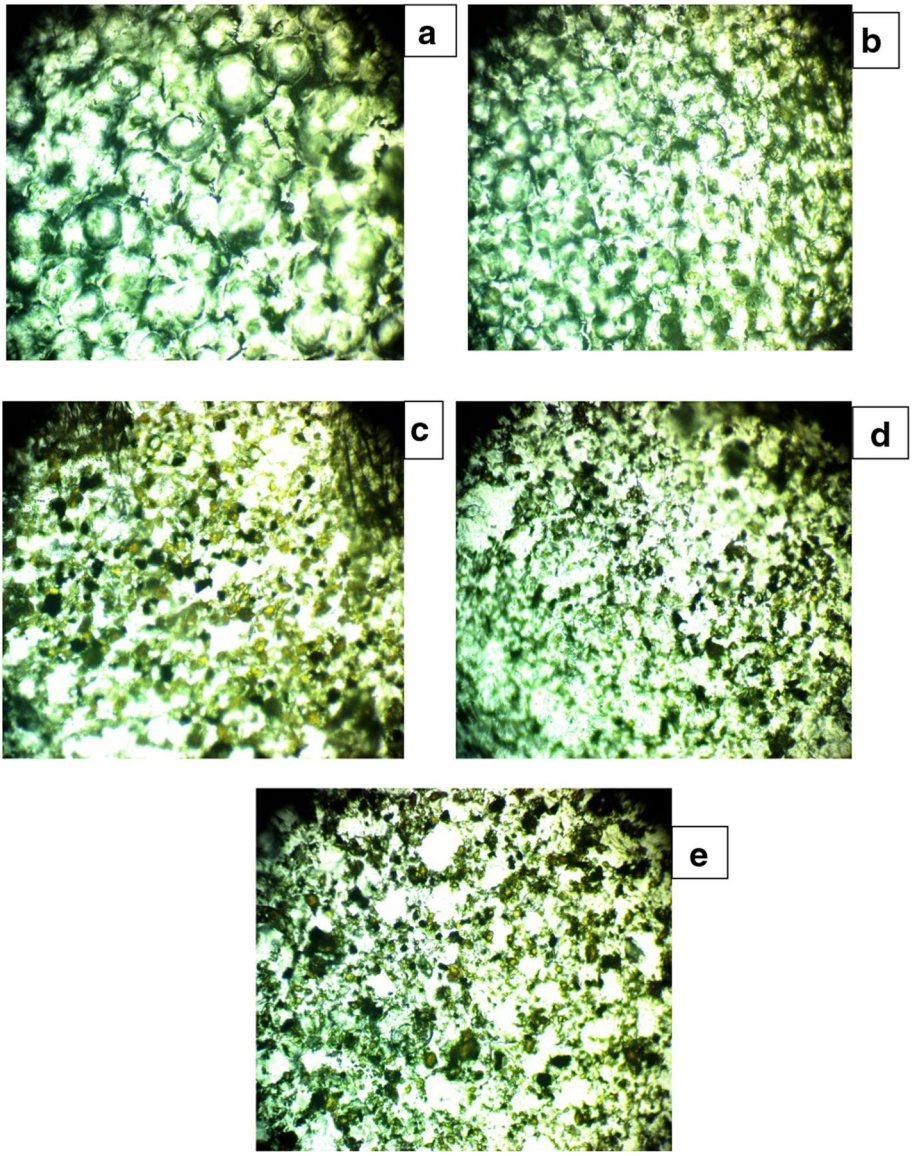

Fig. 2 Photomicrographs 10× for PEO–PVA–$SrTiO_3$–NiO NCs: **a** for PEO–PVA, **b** for 1 wt% $SrTiO_3$–NiO, **c** for 2 wt% $SrTiO_3$–NiO, **d** for 3 wt% $SrTiO_3$–NiO, **e** for 4 wt% $SrTiO_3$–NiO

absorption in the UV range. In the visible range, all nanocomposites have a low absorption. This phenomenon can be explained as interacting with atoms, resulting in photon transmission. The interaction between incident photon and substance occurs as the wavelength decreases, and the photon absorbs. It is very clear from the figure that, As the doping concentration of $SrTiO_3$–NiO nanoparticles is raised, the absorption bands alter, and the band edges shift towards the higher wavelength region with varied absorption strengths. As the weight percentages of nanomaterial's grow, the absorbance rises.

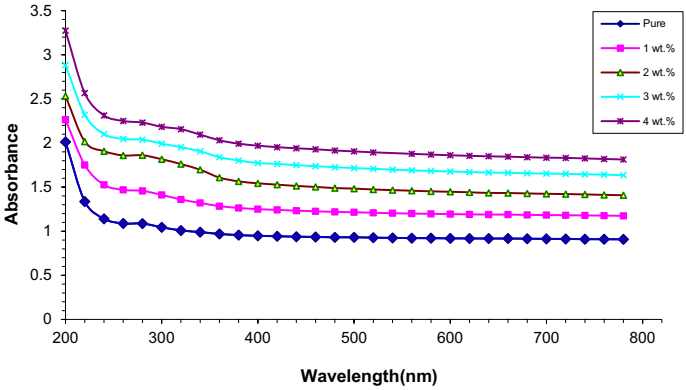

Fig. 3 Difference of absorbance for PEO–PVA–$SrTiO_3$–NiO NCs by wavelength

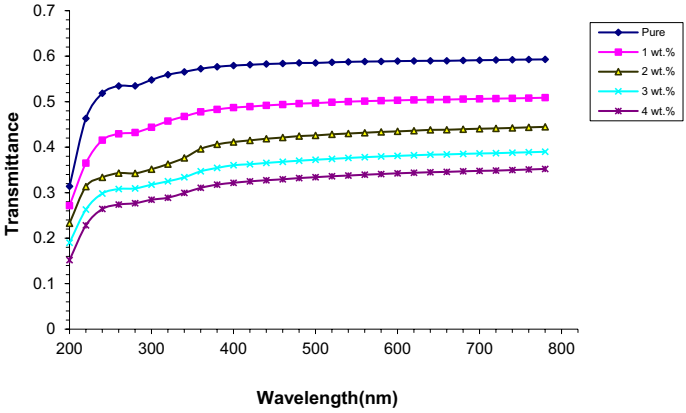

Fig. 4 Difference of transmittance for PEO–PVA–$SrTiO_3$–NiO NCs by wavelength

This is because free electrons absorb the incident light (Alsulami 2021; Chudek et al. 2018; Habeeb et al. 2020).

Figure 4 clarifies the optical transmission spectra for PEO–PVA–$SrTiO_3$–NiO NCs against wavelength.Due to the existence of the PEO–PVA polymer band gap, a substantial drop in transmittance spectrum between 210 and 248 nm was observed (Abbas et al. 2015). (Shown with the doping of PEO–PVA–$SrTiO_3$–NiO NCs polymer solutions, its intensity is continually diminishing. This graph shows unequivocally that the spectrum was changed towards low wave lengths when nano-oxide metals were added to PEO–PVA polymer, which demonstrates that the transmittance spectrum for PEO–PVA–$SrTiO_3$–NiO NCs diminishes as the number of $SrTiO_3$–NiO NPs rises.This is necessary for the electrons in the extra $SrTiO_3$–NiO NPs to capture electromagnetic energy from incoming light and go up to higher energy levels. Since the moving electron fills up open energy band positions and blocks part of incoming light from passing through the material, the process does not result in the emission of radiation.However, since there is not a free electron (i.e., since electrons are attached to atoms by covalent

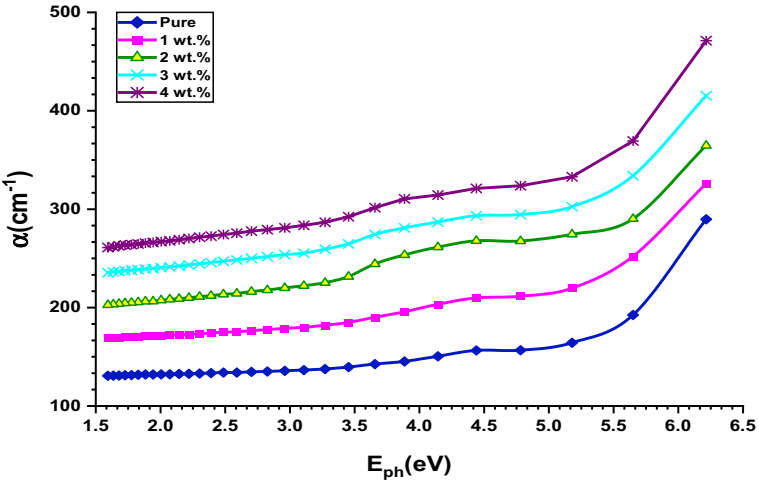

Fig. 5 The absorption coefficient for PEO–PVA–$SrTiO_3$–NiO NCs versus photon energy

bonds), which is required for electron to be broken and moved to conduction band, the PEO–PVA combination has a high transmittance (Sheha et al. 2012).

Figure 5 shows how the absorption coefficient for a PEO–PVA blend with different $SrTiO_3$–NiO NP concentrations relates to photon energy. At low energy levels, there is little absorption, it should be noted. There is a low probability of an electron transition because the input photon's energy is inadequate to move the electron ($h\nu < Eg$) from the valence band to the conduction band. Since absorption increases with energy, there is a good chance that when the input photon's energy is high enough, the electron will transition from the valence band to the conduction band. The incident photon has greater energy than the gap with the forbidden energy, as shown by this example. This shows that the kind of the electron transition may be determined when the absorption coefficient is high ($\alpha > 104$ cm^{-1} at high energy). It is thought that electrons will undergo a straight transition while maintaining their velocity and energy. The opposite, however, is true when the absorption coefficient is low ($\alpha < 104$ cm^{-1}). The value of the acceptable and forbidden indirect transition energy gap will depend on the approved and prohibited indirect transition energy gap in the PEO–PVA combination. The energy gap of the PEO–PVA polymer narrows when the concentration of $SrTiO_3$–NiO nanoparticles in the film's structure rises, leading to the formation of a larger UV absorption peak. Researchers were able to locate the absorption edge using the (α) versus ($h\nu$) curves' linear component to extrapolate to the zero absorption value (Habeeb and Mahdi 2019; Devi et al. 2002). As the $SrTiO_3$–NiO nanoparticle concentration in the PEO–PVA matrix rose, the band edge shrunk. As the absorption edge advances up towards longer wavelengths, the doped sheets' optical band gapgets smaller and narrower. The UV absorption edge shifts as a result of modifications to the electron holes in the conduction and valence bands (Habeeb and Abdul Hamza 2018).

Figure 6 for PEO–PVA–$SrTiO_3$–NiO NCs, the variation of the absorption edge $(\alpha h\upsilon)^{1/2}$ as a function of photon energy is displayed.It has been shown that Eg of nanocompositesdrop with increasing $SrTiO_3$–NiO NPs concentration. The values of permissible energy gap for PEO–PVA–$SrTiO_3$–NiO NCs are due to localization in the prohibited energy gap to high degrees. Indirect transition is suitable for the transition that occurs in the samples. Due

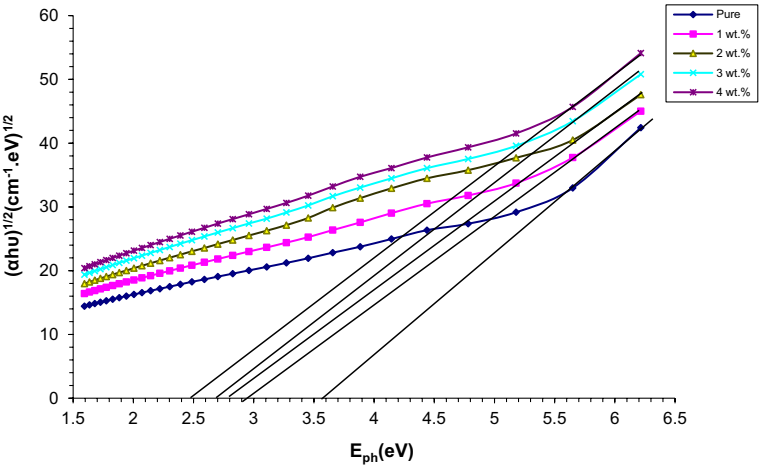

Fig. 6 Relation between photon energy for PEO–PVA–$SrTiO_3$–NiO NCs and $(\alpha h\upsilon)^{1/2}$

to the variety of composites, this behavior occurs (i.e. the electronic conduction depends on added impurities) (Reddy et al. 2006; Yq and Chen 2008). It can be observed from the change of the energy gap for PEO–PVA–$SrTiO_3$–NiO NCs nanocomposites films that the energy gap values decrease as the concentration of $SrTiO_3$–NiO rises. This decrease in the band gap caused by the emergence of new levels made it easier for electrons to go from the valence band to these local levels and into the conduction band, which increased conductivity and reduced the band gap. According to Table 1, a faster addition rate produces polymer routes for electron crossing, which contributes to increased concentration levels in the forbidden energy gap (Varishetty et al. 2010; Hashim et al. 2020).

Figure 7 shows the connection between photon energy and$(\alpha h\upsilon)^{1/3}$by increasing the amount of $SrTiO_3$–NiO NPs in blend the energy gap values for forbidden indirect transitions are reduced, and similarly, these allowed indirect transition values are lower than the forbidden indirect transition values. Table 1 indicates that this attribute contributes to the formation of additional levels as well as electron transitions between the new level tails created by the additive ($SrTiO_3$–CoO)NPs (Alsulami and Rajeh 2021).

Figure 8 shows the relationship between the extinction coefficient of PEO–PVA–$SrTiO_3$–NiO NCs and wavelength. This graph shows that the value of the extinction coefficient increases as $SrTiO_3$–NiO NPs concentration does. Conduct has a high coefficient of absorption as a result. The fluctuation of k values with wavelength indicates that there is some interaction between the medium and the light photons. The percentage

Table 1 Values of energy gap for (allowed and forbidden) indirect transition for PEO–PVA–$SrTiO_3$–NiO NCs

Con. of $SrTiO_3$–NiO NPs wt%	Allowed indirect energy gap (eV)	Forbidden indirect energy gap (eV)
0	3.6	3.8
1	2.9	3.1
2	2.8	2.9
3	2.7	2.7
4	2.5	2.5

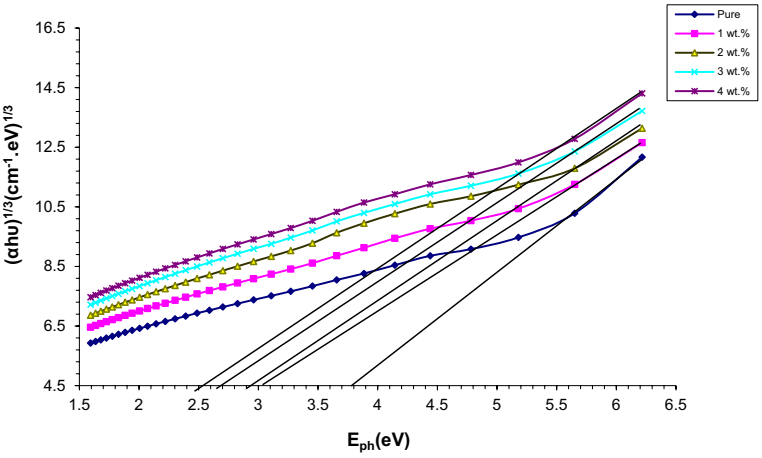

Fig. 7 Relation between the energy of photons for PEO–PVA–$SrTiO_3$–NiO NCs and $(\alpha h\upsilon)^{1/3}$

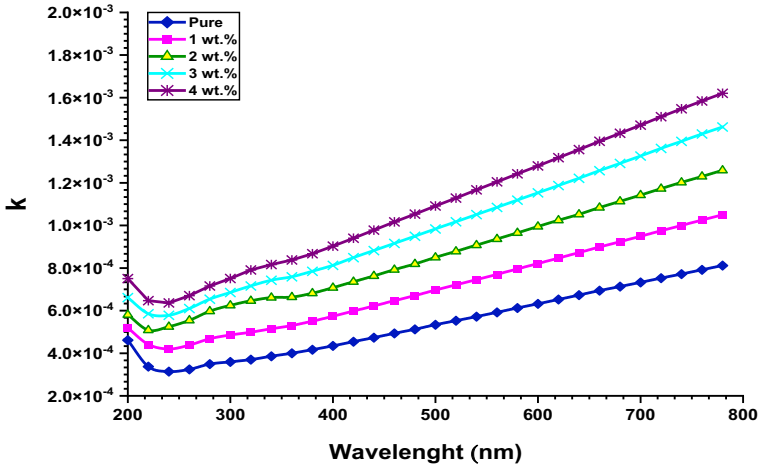

Fig. 8 Relation between extinction coefficient for PEO–PVA–$SrTiO_3$–NiO NCs and wavelength

of electromagnetic energy lost by scattering and absorption per unit thickness in a specific material is known as the extinction coefficient. This figure shows that the extinction coefficient rises at high wavelengths (Habeeb 2014; Habeeb and Hamza 2018; Lee et al. 2006).

Figure 9 PEO–PVA–$SrTiO_3$–NiO NCs have changes in their refractive index and wavelength. One of the reasons for the increase in reflectance PEO–PVA–$SrTiO_3$–NiO NCs is the refractive index increased for the doped samples because the addition of $SrTiO_3$–NiO NPs enhances the intensity of NCs by raising the PEO–PVA blend's refractive index and thereby, increasing the dispersion of the photon event. It is clear that the refractive index displays an area of dispersion at low wavelengths and practically reaches a plateau at high wavelengths. One of a material's most fundamental characteristics is its index of refraction, which is directly tied to its electrical polarizability. The electromagnetic field of the light induces polarization in the molecules, which is reflected by the refractive index. Due to the

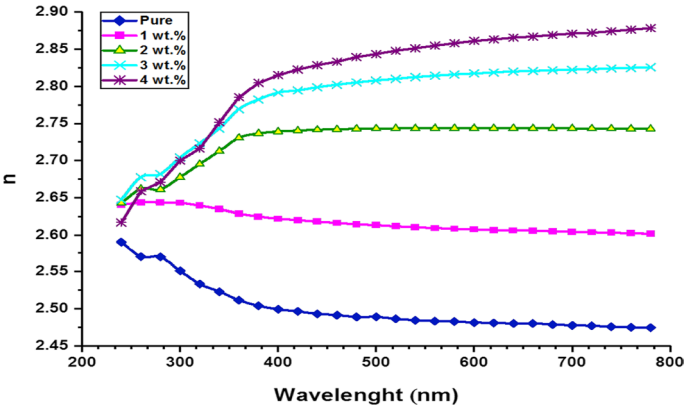

Fig. 9 Refractive index for PEO–PVA–$SrTiO_3$–NiO NCs and wavelength

impact of the electric field component of the incident wave, a material exposed to electromagnetic light will experience time-varying forces inside its internal charge structure. The polar character of the samples was attributed to the broad dispersion area. Polar molecules' inertia prevents them from following the field alternation at high wavelengths (Habeeb and Kadhim 2014; Zhang et al. 2017)

Figures 10 and 11 illustrate the real and imaginary components of the dielectric constant for PEO–PVA–SrTiO–NiO–NiO NCs. The variation of (1) for PEO–PVA–$SrTiO_3$–NiO NCs as a function of wavelength in Fig. 10 indicates the propensity of a material to interact with an electric field and become polarized. The stored energy is associated with the imagined portion, whereas the actual portion discloses the amount by which the substance will reduce the speed of light. Increased $SrTiO_3$–NiO NP concentration alters the imaginary component as a function of wavelength, as seen in Fig. 11. Although the real and imaginary sections display the same pattern of activity, the real component has bigger values. Variable dielectric constants were brought about by interactions between photons and charge carriers in the generated films. A rise in the dielectric constant shows the presence

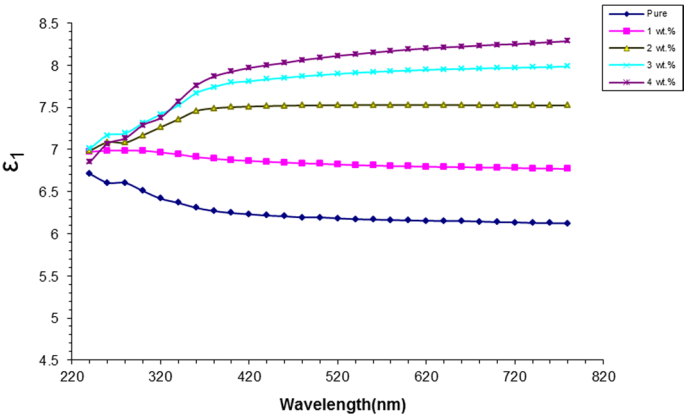

Fig. 10 Difference real part of dielectric constant of PEO–PVA–$SrTiO_3$–NiO NCs with wavelength

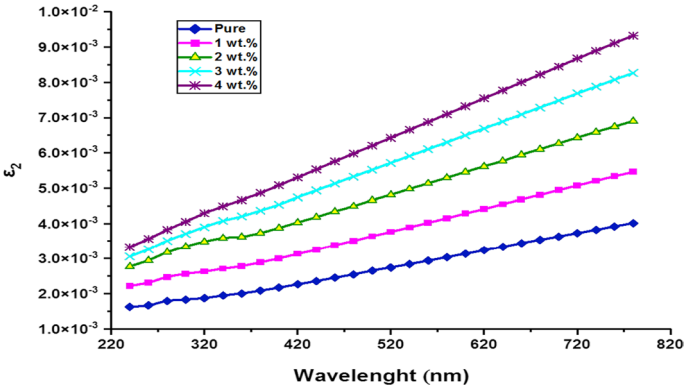

Fig. 11 Difference imaginary part of dielectric constant of PEO–PVA–$SrTiO_3$–NiO NCs with wavelength

of more energy-dense states; this, in turn, causes an increase in polarization, which results in a greater dielectric constant value (Obaid et al. 2013).

Figure 12 illustrates the variety of the optical conductivity of PEO–PVA–$SrTiO_3$–NiO NCs with wavelength. The optical conductivity of all NCs samples diminishes as wavelength rises, which is a characteristic linked to how the optical conductivity varies depending on the wavelength of the light impinging on the NCs sample. The optical conductivity spectra show that all NC samples in this region have high absorbance, which raises optical conductivity at low photon wavelengths and causes the samples to transmit light in the visible and near-infrared spectrum. Along with this, it indicates that more $SrTiO_3$–NiO nanoparticles are produced at greater concentrations, optical conductivity values rise as $SrTiO_3$–NiO concentrations do. The band gap narrows as a result of this increase in conductivity, which is caused by the formation of new local levels in the band gap that make it easier for electrons to move from the valence band to the conduction band. The density of localized stages in the band structure also rises, enhancing optical conductivity and absorption coefficient. Localized levels that have formed in the energy gap are responsible for this behavior in PEO–PVA–$SrTiO_3$–NiONCs (Prabhu et al. 2015; Abutalib and Rajeh 2020).

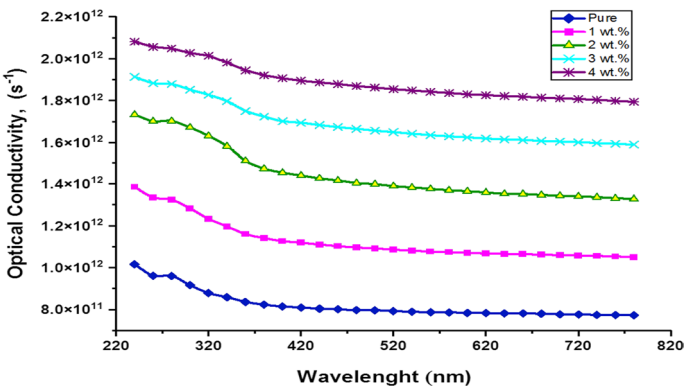

Fig. 12 Difference of optical conductivity for PEO–PVA–$SrTiO_3$–NiO NCs with wavelength

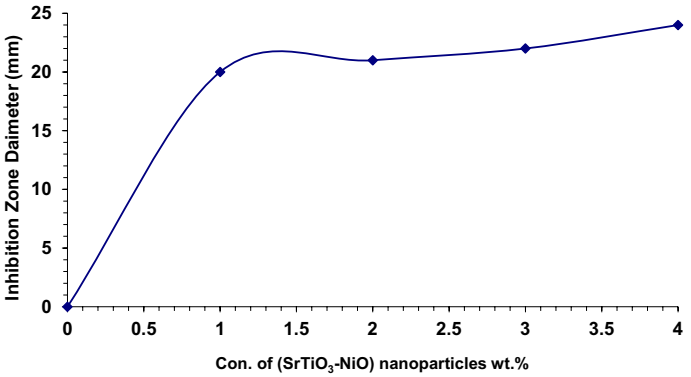

Fig. 13 Antibacterial effect of PEO–PVA blend as a function of $SrTiO_3$–NiO NPs concentrations on *S. aureus*

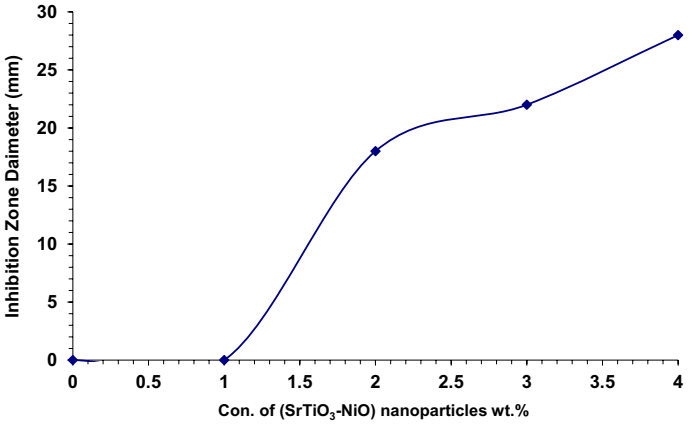

Fig. 14 Antibacterial effect of PEO–PVA blend as a Function of $SrTiO_3$–NiO NPs concentrations on *E. coli*

3.4 Application of PEO–PVA–$SrTiO_3$–NiO NCs antibacterial activity

The antibacterial mechanism is not entirely known, although it differs from nanoparticle to nanoparticle other. While some postulated processes are related to the nanoparticles' physical makeup, such as their potential to damage membranes, others are related to the increased release of antibacterial metal ions from their surfaces. As the particle size lowers, the specific surface area of a dosage of nanoparticles grows, enabling increased material interaction with the environment. Consequently, increasing the surface to volume ratio for materials that are naturally antibacterial improves the antibacterial impact. The release of antibacterial metal ions from the particle surface and the antibacterial physical properties of a nanoparticle related to cell wall penetration or membrane damage are two examples of the various antibacterial mechanisms that an inherently antibacterial material's nanoparticle may possess. The PEO–PVA–$SrTiO_3$–NiO NCs samples were investigated for their antibacterial efficacy against gram positive (S. aureus) and gram negative (pseudomonas fluorescence) bacteria. Figures 13 and 14 demonstrate that when $SrTiO_3$–NiO NP

concentrations increase, the inhibition zone increases. PEO–PVA–$SrTiO_3$–NiO NCs' antibacterial activity might be attributed to reactive oxygen species (ROS) which are created by different NP concentrations. The hydrogen peroxide produced by a chemical interaction between membrane proteins and hydrogen peroxide, which penetrates bacterial cell membranes and destroys the + nanoparticles in NCs and the negative charges on the microbes, may interact electromagnetically, which is another possible mode of action. When the attraction takes shape, the germs oxidize and die. The results showed that the antibacterial activity of PEO–PVA blend was enhanced by the addition of $SrTiO_3$–NiO NPs (Prabhu et al. 2015; Abutalib and Rajeh 2020; Hezma et al. 2019)

4 Conclusion

In the present work, solution cast technique was used to create polymer nanocomposites (PNC_s) based on a PEO–PVA blend. The SEM images show that the surface morphology of PEO–PVA–$SrTiO_3$–NiO NCs films is uniform and consistent, with a random distribution of different pieces or aggregates. Optical microscope images show that the distribution of $SrTiO_3$–NiO NPs additives was homogeneous in the blend and the NPs form a continuous network inside the polymers. Increases in the quantities of $SrTiO_3$–NiO NPs in the PEO–PVA blend lead to increases in absorbance, as well as, absorption coefficient, refractive index, extinction coefficient, dielectric constant (both real and imaginary) and optical conductivity, whereas transmittance decrease. The allowed and forbidden indirect energy gap of this NCs decreased from 3.6 to 2.5 (eV), and from 3.8 to 2.5 (eV) respectively when increasing the weight percentages of NPs to 4 wt%. The diameter of the inhibition zone of *E. coli* and *S. aureusbacteria* increases to 28 and 24 mm respectively as the concentration of $SrTiO_3$–NiO NPs increases. It was evident from the experimental results that enhancement of $SrTiO_3$–NiO nanoparticles is possible through the structural and optical properties and also through the antimicrobial activity of the PEO–PVA blend. This confirms the potential use of these materials in optoelectronics fields such as light filters, transistors sensors diodes, lasers, electronics gates and in food packaging industries.

Acknowledgements Acknowledgments to University of Babylon

Author contributions All authors contributed to the study conception and design. Material preparation, data collection and analysis were performed by SMM and MAH. The first draft of the manuscript was written by MAH and all authors commented on previous versions of the manuscript. All authors read and approved the final manuscript.

Funding No funding.

Availability of data and materials Available.

Declarations

Conflict of interest No conflict of interest.

Consent to participate Consent.

Consent for publication Consent.

Ethical approval The Research is not involving the studies on human or their data.

References

Abbas, N.K., Habeeb, M.A., Algidsawi, A.J.K.: Preparation of chloropenta amine cobalt (III) chloride and study of its influence on the structural and some optical properties of polyvinyl acetate. Int. J. Polym. Sci. **2015**, 926789 (2015). https://doi.org/10.1155/2015/92678

Abutalib, M.M., Rajeh, A.: Preparation and characterization of polyaniline/sodium alginate-doped TiO_2 nanoparticles with promising mechanical and electrical properties and antimicrobial activity for food packaging applications. J. Mater. Sci. Mater. Electron. **31**, 9430–9442 (2020)

Abutalib, M.M., Rajeh, A.: Enhanced structural, electrical, mechanical properties and antibacterial activity of Cs/PEO doped mixed nanoparticles (Ag/TiO_2) for food packaging applications. Polym. Test. **93**, 1–11 (2021). https://doi.org/10.1016/j.polymertesting.2020.107013

Alghamdi, H.M., Abutalib, M.M., Mannaa, M.A., Nur, O., Abdelrazek, E.M., Rajeh, A.: Modification and development of high bioactivities and environmentally safe polymer nanocomposites doped by Ni/ZnOnanohybrid for food packaging applications. J. Mater. Res. Technol. **19**, 3421–3432 (2022a). https://doi.org/10.1016/j.jmrt.2022.06.077

Alghamdi, H.M., Abutalib, M.M., Rajeh, A., Mannaa, M.A., Nur, O., Abdelrazek, E.M.: Effect of the Fe_2O_3/TiO_2 nanoparticles on the structural, mechanical, electrical properties and antibacterial activity of the biodegradable chitosan/polyvinyl alcohol blend for food packaging. J. Polym. Environ. **30**, 3865–3874 (2022b)

Alghamdi, H.M., Abutalib, M.M., Rajeh, A., Mannaa, M.A., Nur, O., Abdelrazek, E.M.: Effect of the on the structural, mechanical, electrical properties and antibacterial activity of the biodegradable chitosan/polyvinyl alcohol blend for food packaging. J. Polym. Environ. **30**, 3865–3874 (2022c)

Alsulami, Q.A.: Structural, dielectric, and magnetic studies based on MWCNTs/$NiFe_2O_4$/ZnO nanoparticles dispersed in polymer PVA/PEO for electromagnetic applications. J. Mater. Sci. Mater. Electron. **32**, 2906–2924 (2021)

Alsulami, Q.A., Rajeh, A.: Synthesis of the SWCNTs/TiO_2 nanostructure and its effect study on the thermal, optical, and conductivity properties of the CMC/PEO blend. Result Phys. **28**, 104675 (2021)

Blythe, T., Bloor, T.D.: Electrical Properties of Polymers, 2nd edn. Cambridge University Press, London (2005)

Chandrakala, H.N., Ramara, B.J., Siddaramaiah, S.: Optical properties and structural characteristics of zinc oxidesinglebondcerium oxide doped polyvinyl alcohol films. J. Alloys Compd. **586**, 333–342 (2014). https://doi.org/10.1016/j.jallcom.2013.09.194

Chang, C.C., Chen, P.H., Chang, C.M.: Preparation and characterization of acrylic polymer–nanogold-nanocomposites from 3-mercaptopropyltrimethoxysilane encapsulated gold nanoparticles. J. Sol-Gel Sci. Technol. **47**, 268–273 (2008). https://doi.org/10.1007/s10971-008-1774-4

Chudek, Z., Apinska, K.L., Wroblewska, A.A., Judek, J., Duzynska, A., Pawlowski, M., Witowski, A.M., Zdrojek, M. (2018) Study of the absorption coefficient of graphene-polymer composites. Sci. Rep. **8**(1), 9132 (2018). https://doi.org/10.1038/s41598-018-27317-0

Devi, C.U., Sharma, A.K., Rao, V.: Electrical and optical properties of pureand silver nitrate-doped polyvinyl alcohol films. Mater. Lett. **56**(3), 167–174 (2002)

Gautam, A., Ram, S.: Preparation and thermo mechanical properties of Ag-PVA nanocomposite films. Mater. Chem. Phys. **119**, 266–271 (2010)

Goswami, A., Bajpai, A.K., Bajpai, J., Sinha, B.K.: Designing vanadiumpent oxide-carboxymethyl cellulose/polyvinyl alcoholbased bionanocomposite films and study of their structure, topography, mechanical, electrical and optical behavior. Polym. Bull. **75**, 807–781 (2017). https://doi.org/10.1007/s00289-017-2067-2

Habeeb, M.A.: Effect of rate of deposition on the optical parameters of GaAs films. Eur. J. Sci. Res. **57**(3), 478–484 (2011)

Habeeb, M.A.: Dielectric and optical properties of (PVAc-PEG-Ber) biocomposites. J. Eng. Appl. Sci. **9**(4), 102–108 (2014). https://doi.org/10.36478/jeasci.2014.102.108

Habeeb, M.A., Abdul Hamza, R.S.: Novel of (biopolymer blend-MgO) nanocomposites: fabrication and characterization for humidity sensors. J. Bionanosci. **12**(3), 328–335 (2018). https://doi.org/10.1166/jbns.2018.1535

Habeeb, M.A., Hamza, R.S.A.: Synthesis of (polymer blend-MgO) nanocomposites and studying electrical properties for piezoelectric application. Indones. J. Electr. Eng. Inform. **6**(4), 428–435 (2018). https://doi.org/10.11591/ijeei.v6i1.511

Habeeb, M.A., Kadhim, W.K.: Study the optical properties of (PVA-PVAC-Ti) nanocomposites. J. Eng. Appl. Sci. **9**(4), 109–113 (2014). https://doi.org/10.36478/jeasci.2014.109.113

Habeeb, M.A., Mahdi, W.S.: Characterization of (CMC-PVP-Fe_2O_3) nanocomposites for gamma shielding application. Int. J. Emerg. Trends Eng. Res. **7**(9), 247–255 (2019). https://doi.org/10.30534/ijeter/2019/06792019

Habeeb, M.A., Hashim, A., Hayder, N.: Structural and optical properties of novel (PS-Cr_2O_3/$ZnCoFe_2O_4$) nanocomposites for UV and microwave shielding. Egypt. J. Chem. **63**, 697–708 (2020). https://doi.org/10.21608/ejchem.2019.12439.1774

Habeeb, M.A., Hashim, A., Hayder, N.: Structural and optical properties of novel (PS-Cr_2O_3/$ZnCoFe_2O_4$) nanocomposites for UV and microwave shielding. Egypt. J. Chem. **63**, 697–708 (2020). https://doi.org/10.21608/ejchem.2019.12439

Hashim, A., Habeeb, M.A., Jebur, Q.M.: Structural, dielectric and optical properties for (polyvinyl alcohol-polyethylene oxide manganese oxide) nanocomposites. Egypt. J. Chem. **63**, 735–749 (2020). https://doi.org/10.21608/ejchem.2019.14849.1901

Hayder, N., Habeeb, M.A., Hashim, A.: Structural, optical and dielectric properties of (PS-In_2O_3/$ZnCoFe_2O_4$) nanocomposites. Egypt. J. Chem. **63**, 577–592 (2020). https://doi.org/10.21608/ejchem.2019.14646.1887

Hezma, A.M., Rajeh, A., Mannaa, M.A.: An insight into the effect of zinc oxide nanoparticles on the structural, thermal, mechanical properties and antimicrobial activity of Cs/PVA composite. Colloids Surf. A Physcochem. Eng. Aspects **581**, 12382 (2019)

Jebur, Q.M., Hashim, A., Habeeb, M.A.: Fabrication, structural and optical properties for (polyvinyl alcohol-polyethylene oxide iron oxide) nanocomposites. Egypt. J. Chem. **63**(2), 611–623 (2020a). https://doi.org/10.21608/ejchem.2019.10197.1669

Jebur, Q.M., Hashim, A., Habeeb, M.A.: Structural, A.C electrical and optical properties of (polyvinyl alcohol-polyethylene oxide-aluminum oxide) nanocomposites for piezoelectric devices. Egypt. J. Chem. **63**, 719–734 (2020b). https://doi.org/10.21608/ejchem.2019.14847.1900

Kumar, K.N., Rao, J.L., Ratnakaram, Y.C.: Optical, magnetic and electricalproperties of multifunctional Cr^{3+}: polyethylene oxide (PEO) polyvinylpyrrolidone (PVP) polymer composites. J. Mol. Struct. **1100**, 546–554 (2015)

Lee, J.K., Lee, Y.J., Chae, W.S., Sung, Y.M.: Enhanced ionic conductivity in PEO-$LiClO_4$ hybrid electrolytes by structural modification. J. Electro. Ceram. **17**, 941–944 (2006)

Luo, J., Chu, W., Sall, S., Petit, C.: Facile synthesis of monodispersed Au nanoparticles-coated on Stöber silica. Colloids Surf. A **425**, 83–91 (2013). https://doi.org/10.1016/j.colsurfa.2013.02.056

Mahdi, S.M., Habeeb, M.A.: Evaluation of the influence of $SrTiO_3$ and CoO nanofillers on the structural and electrical polymer blend characteristics for electronic devices. Digest J. Nanomater. Biostruct. **17**(3), 941–948 (2022). https://doi.org/10.15251/DJNB.(2022).173.941

McKee, R.A., Walker, F.J., Chisholm, M.F.: Crystalline oxides on silicon: the first five monolayers. Phys. Rev. Lett. (1998). https://doi.org/10.1103/PhysRevLett.81.3014

Obaid, H.N., Habeeb, M.A., Rashid, F.L., Hashim, A.: Thermal energy storage by nanofluids. J. Eng. Appl. Sci. **8**(5), 143–145 (2013). https://doi.org/10.36478/jeasci.2013.143.145

Pattabi, M., Amma, B.S., Manzoor, K., Mater, J.: Optical parameters of $AgNO_3$ doped poly(vinyl alcohol) films. Res. Bull. **24**, 828–835 (2007)

Prabhu, Y.T., Rao, K.V., Siva Kumari, B.V., Kumar, S.S., Pavani, T.: synthesis of Fe_3O_4 nanoparticles and its antibacterial application. Int. Nano Lett. **5**(2), 85–92 (2015). https://doi.org/10.1007/s40089-015-0141-z

Reddy, C.V.S., Zhu, L.Q., Mai, W.: Optical, electrical and discharge profiles for (PVC+ NaIO4) polymer electrolytes. J. Appl. Electrochem. **36**, 1051–1056 (2006). https://doi.org/10.1007/s10800-006-9158-3

Selvi, J., Mahalakshmi, S., Parthasarathy, V.: Synthesis, structural, optical, electrical and thermal studies of polyvinyl alcohol/CdO nanocomposite films. J. Inorg. Organomet. Polym. Mater. **27**, 1918–1926 (2017)

Shankar, U.V., Dubey, S.K., Arvind, S., Tripathi, S.: Structural, optical and morphological properties of PVA/Fe_2O_3 nanocomposite thin films. IJCPS **3**, 43–48 (2014)

Sheha, E., Khoder, H., Shanap, T.S., El-Shaarawy, M., El Mansy, M.K.: Structure, dielectric and optical properties of p-type (PVA/CuI) nanocomposite polymer electrolyte for photovoltaic cells. Univ. Benha. Egypt. **123**(13), 1161–1166 (2012)

Tintu, R., Saurav, K., Sulakshna, K., Nampoori, V.P., Radhakrishnan, N.P., Thomas, S.: Ge28Se60Sb12/PVA composite films for photonic applications. J. Non-Oxide Glas. **2**(4), 167–174 (2010)

Varishetty, M.M., Qiu, W., Gao, Y., Chen, W.: Structure, electrical and optical properties of (PVA/LiAsF6) polymer composite electrolyte films. Polym. Eng. Sci. (2010). https://doi.org/10.1002/pen.21437

Yq, R., Chen, S.: Molecular composites comprising TiO2 and their optical properties. Macromolecules **41**, 4838–4844 (2008). https://doi.org/10.17656/jzs.10546

Zhang, L., Jiang, Y., Ding, Y., Povey, M., York, D.: Investigation into the antibacterial behaviour of suspensions of ZnO nanoparticles (ZnO nanofluids). J. Nanopart. Res. **9**(3), 479–4891 (2017)